Large Angular Jump Mechanism Observed for Hydrogen Bond Exchange in Aqueous Perchlorate Solution

Minbiao Ji, *et al.*

Science **328**, 1003 (2010);
DOI: 10.1126/science.1187707

This copy is for your personal, non-commercial use only.

If you wish to distribute this article to others, you can order high-quality copies for your colleagues, clients, or customers by clicking here.

Permission to republish or repurpose articles or portions of articles can be obtained by following the guidelines here.

The following resources related to this article are available online at www.sciencemag.org (this information is current as of May 20, 2010):

Updated information and services, including high-resolution figures, can be found in the online version of this article at:
http://www.sciencemag.org/cgi/content/full/328/5981/1003

Supporting Online Material can be found at:
http://www.sciencemag.org/cgi/content/full/328/5981/1003/DC1

This article **cites 24 articles**, 10 of which can be accessed for free:
http://www.sciencemag.org/cgi/content/full/328/5981/1003#otherarticles

This article has been **cited by** 1 articles hosted by HighWire Press; see:
http://www.sciencemag.org/cgi/content/full/328/5981/1003#otherarticles

This article appears in the following **subject collections**:
Chemistry
http://www.sciencemag.org/cgi/collection/chemistry

Science (print ISSN 0036-8075; online ISSN 1095-9203) is published weekly, except the last week in December, by the American Association for the Advancement of Science, 1200 New York Avenue NW, Washington, DC 20005. Copyright 2010 by the American Association for the Advancement of Science; all rights reserved. The title *Science* is a registered trademark of AAAS.

Large Angular Jump Mechanism Observed for Hydrogen Bond Exchange in Aqueous Perchlorate Solution

Minbiao Ji,[1,2] Michael Odelius,[3] K. J. Gaffney[1]*

The mechanism for hydrogen bond (H-bond) switching in solution has remained subject to debate despite extensive experimental and theoretical studies. We have applied polarization-selective multidimensional vibrational spectroscopy to investigate the H-bond exchange mechanism in aqueous $NaClO_4$ solution. The results show that a water molecule shifts its donated H-bonds between water and perchlorate acceptors by means of large, prompt angular rotation. Using a jump-exchange kinetic model, we extracted an average jump angle of 49 ± 4°, in qualitative agreement with the jump angle observed in molecular dynamics simulations of the same aqueous $NaClO_4$ solution.

Hydrogen bonds (H-bonds) provide the intermolecular adhesion that dictates the unique properties of liquid water and aqueous solutions. Although H-bonds constrain the local ordering and orientation of molecules in solution, these local H-bond networks disband and reform on the picosecond time scale. This structural lability critically influences chemical and biological transformations. Our understanding of the dynamics of hydrogen bond dissociation and reformation has been transformed by the union of ultrafast vibrational spectroscopy and molecular dynamics simulations (*1*–*14*), but the detailed mechanism for H-bond switching in aqueous solution remains uncertain. Recent simulation studies of water and aqueous ionic solutions have proposed that H-bond exchange involves large angular jumps of 60° to 70° (*1*, *5*). However, the substantial complexities inherent in simulating the structural and dynamical properties of water highlight the importance of validating this proposal experimentally.

Two-dimensional infrared (2D-IR) spectroscopy provides an excellent opportunity to study this class of ultrafast chemical exchange (*15*–*19*). We applied a variation of this technique (Fig. 1) to directly investigate the orientational jump mechanism for H-bond switching in aqueous ionic solutions. The dissolution of $NaClO_4$ in isotopically mixed water generates two deuterated hydroxyl (OD) stretch frequencies: OD groups donating a H-bond to another water molecule (OD_W) absorb at 2534 cm^{-1}, whereas OD groups donating a H-bond to a perchlorate anion (OD_P) absorb at 2633 cm^{-1} (Fig. 1D). This spectroscopic distinction between the OD_W and OD_P provides the opportunity to track H-bond exchange by monitoring the growth in the cross-peak intensity in the time-dependent 2D spectra (*3*, *4*), as shown in Fig. 1. Recent studies by Moilanen *et al.* (*3*) and Park *et al.* (*4*) have used this attribute of the water hydroxyl stretch to measure the H-bond exchange rate in aqueous $NaBF_4$ and $NaClO_4$ solutions. These experiments measured the exchange between water-water and water-anion H-bond configurations but did not directly address the hydroxyl group reorientation associated with H-bond exchange.

Two advances implemented in the present study have allowed us to extract the orientational jump angle associated with H-bond exchange. First, we have measured the laser polarization dependence of the 2D-IR spectra (*20*). Polarization-selective vibrational pump-probe measurements have been widely used to study the orientational dynamics of water molecules (*6*, *7*), but these measurements cannot distinguish which water molecules have exchanged their H-bonding configuration. This can only be achieved by introducing an additional spectral dimension. Our work extends previous polarization-selective 2D-IR studies of the relative orientation of coupled vibronic states (*21*, *22*); specifically, we address the time-dependent change in orientation of the vibrationally excited hydroxyl groups induced by chemical exchange. The second advance is a modification of the kinetic model (*23*) used to interpret 2D-IR spectra, so as to include vibrational transition dipole moment jump-reorientation induced by chemical exchange. Previous data analysis assumed H-bond exchange did not induce jump-reorientation (*3*, *4*).

2D-IR spectroscopy monitors equilibrium H-bond switching dynamics on a picosecond time scale (*15*–*19*) by labeling molecules through resonant excitation at their OD stretch frequencies and then correlating these initial frequencies (ω_τ) with the (potentially shifted) stretch frequencies (ω_m) associated with these same molecules after an experimentally controlled waiting time (T_W). Thus, 2D-IR can determine when a vibrationally labeled OD_W hydroxyl group converts to an OD_P configuration during T_W. The cross-peak only reflects H-bond exchange events in which the hydroxyl group switches between the OD_W and OD_P configurations. By adding polarization selectivity, we furthermore access the orientational dynamics of water molecules that have switched between OD_W and OD_P configurations. In the polarization-selective 2D-IR measurement, the first two pulses that control the frequency labeling of OD stretches have parallel polarizations that preferentially excite transition dipole moments parallel to the excitation polarization. During the T_W waiting time, the excited molecules randomize their orientation in addition to undergoing H-bond exchange between the OD_W and OD_P configurations (Fig. 1A). If the H-bond exchange only minimally perturbs the orientation of the vibrationally excited hydroxyl group, then both the diagonal and the cross-peak intensities will exhibit similar polarization dependence. However, if the molecules exchange via large angular jumps, the cross-peak signal that results solely from OD_W-OD_P exchanged populations will show distinctly different polarization dependence from the diagonal peaks (Fig. 1, B and C).

Figure 2 shows the T_w-dependent polarization-selective 2D-IR spectra for aqueous 6M $NaClO_4$. The positive peaks shown in red along the diagonal ($\omega_\tau = \omega_m$) result from the fundamental vibrational transition ($\upsilon = 0 \rightarrow 1$) within each H-bond configuration. We label the peak volumes $I_{llmm}^{(ij)}$ for the diagonal ($i = j$) and the off diagonal ($i \neq j$) peaks: i and j refer to the H-bond configurations associated with ω_τ and ω_m, and l and m refer to the laser polarization. The cross-peak at $(\omega_\tau,\omega_m) = (2534,2633)\,cm^{-1}$ results from OD_W switching to OD_P, $I_{llmm}^{(WP)}$. Because this H-bond exchange occurs at equilibrium, the exchange process from OD_P to OD_W will also generate a cross-peak $I_{llmm}^{(PW)}$ at $(\omega_\tau,\omega_m) = (2633,2534)\ cm^{-1}$ with $I_{llmm}^{(PW)} = I_{llmm}^{(WP)}$. Experimentally, the $\upsilon = 1 \rightarrow 2$ excited state absorption of OD_P obscures this cross-peak (*4*), so we use the $I_{llmm}^{(WP)}$ signal to characterize the jump angle. The vibrationally excited molecules that have switched between the OD_P and OD_W configurations project nearly equivalent signal intensities for perpendicular and parallel polarizations. As will be shown, this equivalence reflects the large angular jumps that lead to H-bond switching.

Figure 3 further highlights the polarization-dependent population dynamics by comparing the peak volumes for the isotropic ($I_{iso}^{(ij)} = I_{zzzz}^{(ij)} + 2I_{zzyy}^{(ij)}$) and anisotropic ($I_{aniso}^{(ij)} = I_{zzzz}^{(ij)} - I_{zzyy}^{(ij)}$) signals for a diagonal-peak ($ij = PP$) and a cross-peak ($ij = WP$). The $I_{iso}^{(PP)}$ signal reflects the population decay of the OD_P configuration, whereas $I_{aniso}^{(PP)}$ reflects population relaxation and orientational randomization of the OD_P configuration. The $I_{iso}^{(WP)}$ signal rise time reflects the rate of H-bond switching, whereas the decay results primarily from OD_P population relaxation. Unlike previous measurements of the H-bond switching time (*3*, *4*), $I_{iso}^{(ij)}$ decouples the orientational dynamics from the H-bond configurational switching and so provides a superior measure of the exchange rate. The $I_{aniso}^{(WP)}$ signal clearly shows the very small dependence of

---

[1] PULSE Institute for Ultrafast Energy Science, SLAC National Accelerator Laboratory, Stanford University, Stanford, CA 94305, USA. [2] Department of Physics, Stanford University, Stanford, CA 94305, USA. [3] Fysikum, AlbaNova University Center, Stockholm University, SE-106 91 Stockholm, Sweden.

*To whom correspondence should be addressed. E-mail: kgaffney@slac.stanford.edu

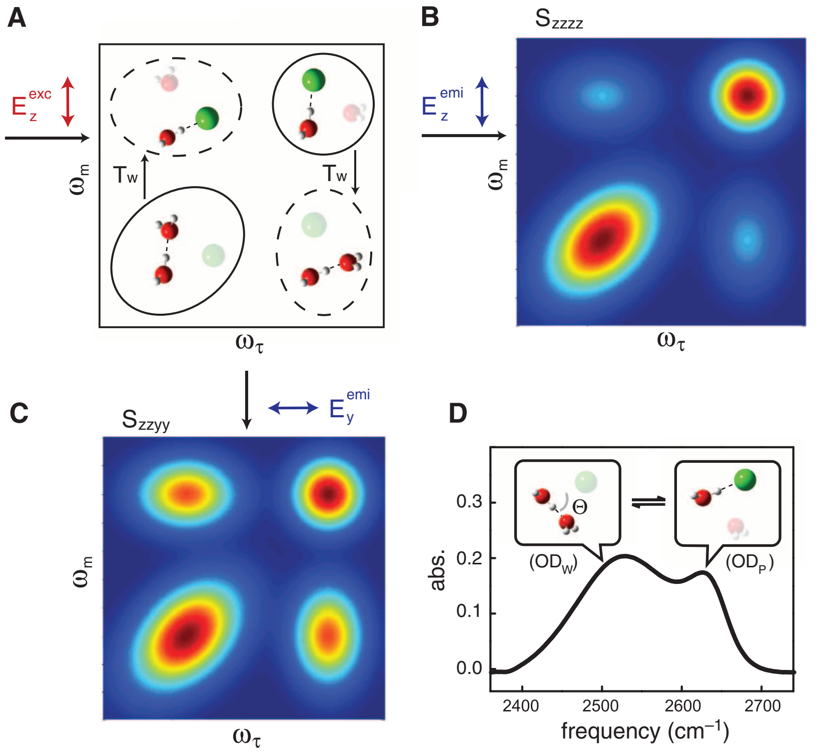

Fig. 1. Interpretation of polarization-selective 2D-IR signals. The H-bond configurations appear schematically, with the green spheres representing perchlorate ions. **(A)** Linearly polarized excitation pulses selectively label vibrational dipoles oriented parallel to the z direction, as shown in the diagonal regions of the 2D spectra. After a T_W waiting time, vibrationally labeled hydroxyl groups that have not changed H-bond configuration contribute to the diagonal component of the 2D-IR signal with minimal reorientation of the OD transition dipole. Vibrationally labeled hydroxyl groups that have undergone H-bond exchange generate cross-peak spectral intensity. If the exchange proceeds through large angular jumps, the hydroxyl groups associated with the cross-peaks will show markedly different polarization dependence than those resonating along the diagonal. This can be seen most clearly by comparing the ratio of cross-peak and diagonal-peak intensities generated with **(B)** all parallel laser polarizations (S_{zzzz}, E_z^{exc}, E_z^{emi}) and **(C)** cross-polarized laser pulses (S_{zzyy}, E_z^{exc},E_y^{emi}). **(D)** Fourier transform IR (FTIR) absorption spectrum for 6M $NaClO_4$ dissolved in H_2O containing 5% monodeuterated water. The lower frequency peak at 2534 cm^{-1} corresponds to the OD stretch donating a H-bond to other water molecules (OD_W); the peak at 2633 cm^{-1} corresponds to the OD stretch donating a H-bond to a perchlorate ion (OD_P).

the cross-peak intensity on the laser polarization. The method used to extract the peak volumes can be found elsewhere (*3*, *23*).

We modeled the polarization-selective 2D-IR spectra using diagrammatic perturbation theory and an angular jump-exchange kinetic model. This provides a framework for interpreting the time (T_W) and angle (Ω) dependent excited state population $N_i(T_W)$, orientation, and spectral diffusion dynamics (*20*, *23*, *24*). The simplest variant of the angular jump-exchange kinetic model presumes that an orientational jump through angle Θ accompanies H-bond exchange between the OD_W and OD_P configurations, whereas reorientation of hydroxyl groups occurs diffusively within a particular H-bond configuration. The model requires the angular rate of change during an angle jump to be much larger than the angular rate of change induced by orientational diffusion. As will be discussed, this requirement is consistent with our experimental and simulation results.

The angular jump-exchange kinetic model attributes the dynamics to (i) population decay with decay rates k_W and k_P, (ii) orientational diffusion with diffusion constants D_W and D_P, and (iii) chemical exchange with rate constants $k_{W\text{-}P}$ and $k_{P\text{-}W}$ and a H-bond exchange jump angle Θ. This model leads to ensemble-averaged populations as a function of T_W and laser polarization. For the S_{zzzz} and S_{zzyy} geometries, the polarization-dependent populations can be expressed as in Eqs. 1 and 2.

$$\begin{pmatrix} N_W(T_W) \\ N_P(T_W) \end{pmatrix}_{zzzz} = \left(e^{-A\cdot T_w} + \frac{4}{5}e^{-B\cdot T_W}\right) \times \frac{1}{3}\begin{pmatrix} N_W(0) \\ N_P(0) \end{pmatrix} \qquad (1)$$

$$\begin{pmatrix} N_W(T_W) \\ N_P(T_W) \end{pmatrix}_{zzyy} = \left(e^{-A\cdot T_w} - \frac{2}{5}e^{-B\cdot T_W}\right) \times \frac{1}{3}\begin{pmatrix} N_W(0) \\ N_P(0) \end{pmatrix} \qquad (2)$$

A and B correspond to matrices that contain all the kinetic coefficients, as well as Θ,

$$A = \begin{pmatrix} k_W + k_{W-P} & -k_{P-W} \\ -k_{W-P} & k_P + k_{P-W} \end{pmatrix},$$

$$B = \begin{pmatrix} k_W + k_{W-P} + 6D_W & -\langle P_2(\cos\Theta)\rangle k_{P-W} \\ -\langle P_2(\cos\Theta)\rangle k_{W-P} & k_P + k_{P-W} + 6D_P \end{pmatrix}$$

where $P_2(\cos\Theta) = (3\cos^2\Theta - 1)/2$ and $\langle\ldots\rangle$ corresponds to an ensemble average. These equations reduce to the exchange kinetic model of Kwak *et al.* (*23*) when Θ = 0° and can be straightforwardly related to the theory of coupled vibrations developed by Golonzka and Tokmakoff (*21*). The A matrix has no orientational dependence and contributes solely to $I_{iso}^{(ij)}$ with dynamics determined by the excited state lifetime and the chemical exchange rate. The B matrix contributes solely to $I_{aniso}^{(ij)}$ with dynamics determined by Θ, D_W, and D_P. As shown in the supporting text, a large jump angle leads to a small $\langle P_2(\cos\Theta)\rangle$ value and the very small cross-peak anisotropy measured experimentally. We have chosen to present the simplest variant of the jump-exchange kinetic model for conceptual clarity, but we have also investigated more sophisticated models. In the supporting text, we discuss three critical aspects of the model and demonstrate that the extracted Θ value is fundamentally insensitive to the distribution of jump angles, the time evolution of the jump angle, and the detailed dynamics of the orientational randomization for hydroxyl groups that remain in a given H-bond configuration.

We used numerical response function calculations based on the above model to analyze the experimental data. The calculated anisotropic spectra appear in Fig. 2D. We used standard methods to obtain starting values for the vibrational relaxation, orientational diffusion, and frequency-frequency correlation function parameters (*4*, *23*). The fitting of the polarization-selective 2D-IR spectra allow the extraction of the H-bond exchange rate $k_{W\text{-}P}$ and jump angle Θ. The analysis uses global fitting of the polarization-selective 2D-IR spectra for T_W times of 0.2, 1, 2, 3, 4, 5, and 7 ps. Fitting results give Θ = 49 ± 4°, $(6D_W)^{-1} = 5 \pm 0.5$ ps, $(6D_P)^{-1} = 4.6 \pm 0.5$ ps, $(k_{P-W})^{-1} = 9 \pm 1$ ps, $(k_{W-P})^{-1} = 18 \pm 2$ ps, and a total exchange rate of $\tau_{ex} = (k_{P-W} + k_{W-P})^{-1} = 6 \pm 1$ ps, consistent with our previous result (*4*). We also fit the T_W-dependent $I_{iso}^{(ij)}$ and $I_{aniso}^{(ij)}$ peak volumes, as shown in Fig. 3. These fitting results agree with the response function global fitting, within experimental error. Within the angular jump-exchange kinetic model, only large values of Θ, D_W, and D_P could lead to the very small anisotropy of the cross-peak $I_{aniso}^{(WP)}$, but the anisotropy of the diagonal peaks greatly constrains D_W and D_P. These constraints, as well as the high sensitivity of the cross-peak anisotropy to small changes in the jump angle around 49°, render the Θ value extracted from the measurements robust.

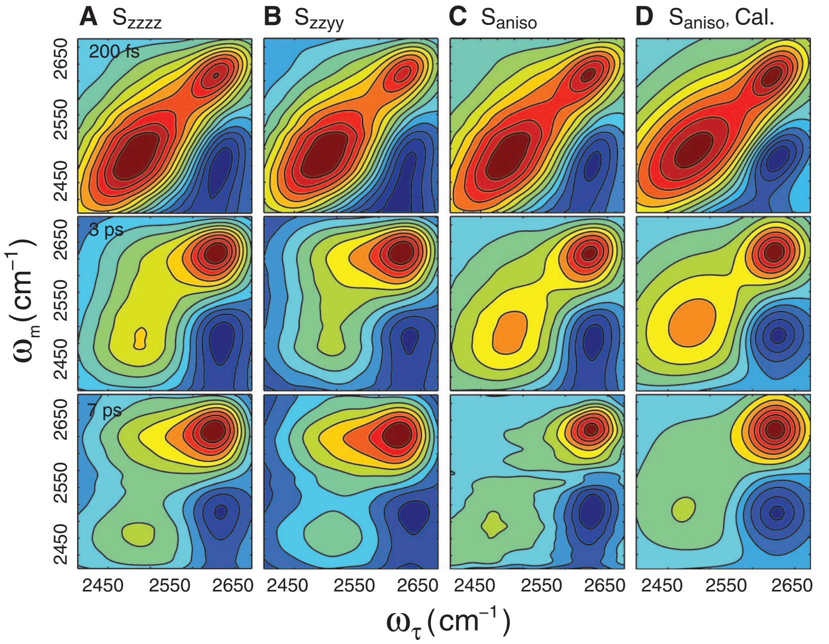

Fig. 2. Normalized polarization-selective 2D-IR spectra at T_W = 0.2, 3, and 7 ps. (**A**) Parallel polarization spectra (S_{zzzz}), (**B**) perpendicular polarization spectra (S_{zzyy}), and (**C**) anisotropic spectra, ($S_{aniso} = S_{zzzz} - S_{zzyy}$). Peak assignments can be found in the text. The cross-peaks show very little anisotropy compared with the diagonal peaks (C), clearly indicating that large-angle rotation of hydroxyl groups accompanies H-bond switching. (**D**) Calculated anisotropic spectra based on Eqs. 1 and 2.

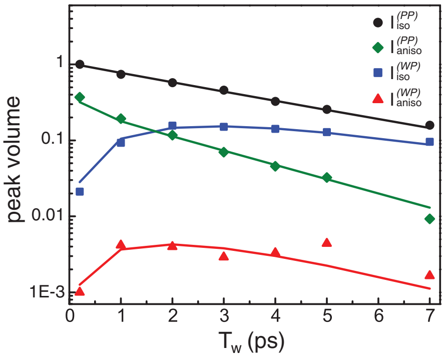

Fig. 3. Logarithmic plot of the polarization-selective peak volumes for the isotropic, $I_{iso}^{(ij)} = I_{zzzz}^{(ij)} + 2I_{zzyy}^{(ij)}$, and anisotropic, $I_{aniso}^{(ij)} = I_{zzzz}^{(ij)} - I_{zzyy}^{(ij)}$, signals for the $ij = PP$ diagonal-peak and the $ij = WP$ cross-peak. The solid lines give the kinetic model fit to the data with a H-bond exchange rate of 6 ± 1 ps and a jump angle of 49 ± 4°.

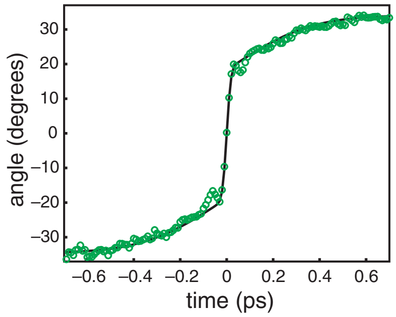

Fig. 4. CPMD simulation of the jump angle for H-bond exchange between the OD_P and the OD_W configurations for aqueous 6 M $NaClO_4$ solution. The data have been fit with a sum of two error functions (solid line). Results show the change in angle proceeding with two time constants, 50 fs for an initial 40° angular jump and 1 ps for a slower 27° angular rotation.

We also performed Car-Parrinello molecule dynamics (CPMD) simulations (*25*) of aqueous 6M $NaClO_4$ to complement our experimental studies (*20*). The CPMD methodology differs substantially from that used previously (*1*, *5*, *14*) to study H-bond switching, yet as shown in Fig. 4, very similar angular jump dynamics emerge in the CPMD simulations of H-bond switching between OD_P and OD_W configurations (*1*, *5*). Analysis of the mean trajectory indicates that the orientation changes on two time scales, with a 40° jump occurring with a 50-fs time constant and a 27° reorientation occurring with a 1-ps time constant. By simulating the same solution as that studied experimentally, we can make a direct comparison between experiment and simulation. The results of the simulation qualitatively agree with our experimental results, validating the angular jump mechanism for H-bond switching in aqueous $NaClO_4$ solutions. The time constant for the fast component resembles the period of a water librational motion, consistent with the assessment that the orientational jump reflects a primarily concerted rotational motion. The 1-ps process occurs too slowly to be viewed as concerted, but our experiment cannot accurately measure the detailed time evolution of the angular jump because the cross-peak intensity grows in with $\tau_{ex} = 6$ ps. Nonetheless, for $T_W \leq 2$ ps, the cross-peak shows a very small anisotropy (fig. S8), which has been accurately modeled with an impulsive angular jump and conforms to the predominantly subpicosecond angular dynamics observed in the simulation. Whether the lack of quantitative agreement between experiment and simulation reflects limitations in the CPMD simulation or the modeling of the experimental data awaits further investigation.

References and Notes

1. D. Laage, J. T. Hynes, *Proc. Natl. Acad. Sci. U.S.A.* **104**, 11167 (2007).
2. C. J. Fecko, J. D. Eaves, J. J. Loparo, A. Tokmakoff, P. L. Geissler, *Science* **301**, 1698 (2003).
3. D. E. Moilanen, D. Wong, D. E. Rosenfeld, E. E. Fenn, M. D. Fayer, *Proc. Natl. Acad. Sci. U.S.A.* **106**, 375 (2009).
4. S. Park, M. Odelius, K. J. Gaffney, *J. Phys. Chem. B* **113**, 7825 (2009).
5. D. Laage, J. T. Hynes, *Science* **311**, 832 (2006).
6. Y. L. A. Rezus, H. J. Bakker, *J. Chem. Phys.* **123**, 114502 (2005).
7. H. J. Bakker, *Chem. Rev.* **108**, 1456 (2008).
8. C. P. Lawrence, J. L. Skinner, *J. Chem. Phys.* **118**, 264 (2003).
9. J. B. Asbury *et al.*, *J. Phys. Chem. A* **108**, 1107 (2004).
10. J. D. Eaves *et al.*, *Proc. Natl. Acad. Sci. U.S.A.* **102**, 13019 (2005).
11. M. L. Cowan *et al.*, *Nature* **434**, 199 (2005).
12. B. Nigro, S. Re, D. Laage, R. Rey, J. T. Hynes, *J. Phys. Chem. A* **110**, 11237 (2006).
13. A. Luzar, D. Chandler, *Phys. Rev. Lett.* **76**, 928 (1996).
14. R. Ludwig, *Chem. Phys. Chem.* **8**, 44 (2007).
15. J. F. Cahoon, K. R. Sawyer, J. P. Schlegel, C. B. Harris, *Science* **319**, 1820 (2008).
16. J. Zheng *et al.*, *Science* **309**, 1338 (2005).
17. J. Zheng, K. Kwak, J. Xie, M. D. Fayer, *Science* **313**, 1951 (2006).
18. S. Woutersen, Y. Mu, G. Stock, P. Hamm, *Chem. Phys.* **266**, 137 (2001).
19. Y. S. Kim, R. M. Hochstrasser, *Proc. Natl. Acad. Sci. U.S.A.* **102**, 11185 (2005).
20. Methods are detailed in supporting online material at *Science* Online.
21. O. Golonzka, A. Tokmakoff, *J. Chem. Phys.* **115**, 297 (2001).
22. M. T. Zanni, N. H. Ge, Y. S. Kim, R. M. Hochstrasser, *Proc. Natl. Acad. Sci. U.S.A.* **98**, 11265 (2001).
23. K. Kwak, J. Zheng, H. Cang, M. D. Fayer, *J. Phys. Chem. B* **110**, 19998 (2006).
24. A. Tokmakoff, *J. Chem. Phys.* **105**, 1 (1996).
25. R. Car, M. Parrinello, *Phys. Rev. Lett.* **55**, 2471 (1985).
26. M.J. and K.J.G. were supported through the PULSE Institute at the SLAC National Accelerator Laboratory by the U.S. Department of Energy Office of Basic Energy Sciences. M.O. acknowledges support from the Carl Tryggers and Magnus Bergwall foundations and the Swedish Research Council, and computer time allocations at the Swedish National Supercomputer Center and Center for Parallel Computing (PDC).

Supporting Online Material

www.sciencemag.org/cgi/content/full/328/5981/1003/DC1
Materials and Methods
Figs. S1 to S11
Table S1
References

29 January 2010; accepted 16 March 2010
10.1126/science.1187707